J. Membrane Biol. 196, 83–94 (2003)
DOI: 10.1007/s00232-003-0627-x

The Journal of
Membrane
Biology

Inhibition of the Endogenous Volume-regulated Anion Channel (VRAC) in HEK293 Cells by Acidic Di-Aryl-Ureas

N. Hélix, D. Strøbaek, B.H. Dahl, P. Christophersen
NeuroSearch A/S, Pederstrupvej 93, DK-2750, Ballerup, Denmark

Received: 7 May 2003/Revised: 8 September 2003

Abstract. The endogenous volume-regulated anion channel (VRAC) from HEK293 cells was pharmacologically characterized using the whole-cell patch-clamp technique. Under isotonic conditions a small (1.3 nS), Ca^{2+}-independent Cl conductance was measured. However, swelling at 75% tonicity activated a VRAC identified as an outward-rectifying anion current ($P_I > P_{Cl} > P_{gluconate}$), which was ATP-dependent and showed inactivation at positive potentials. Activation of this current followed a sigmoid time course, reaching a plateau conductance of 42.6 nS after 12–15 min ($t_{1/2}$ = 7 min). The pharmacology of this VRAC was investigated using standard Cl^--channel blockers (NPPB, DIDS, and tamoxifen) as well as a new group (acidic di-aryl ureas) of Cl^--channel blockers (NS1652, NS3623, NS3749, and NS3728). The acidic di-aryl ureas were originally synthezised for inhibition of the human erythrocyte Cl^- conductance in vivo. NS3728 was the most potent VRAC blocker in this series (IC_{50} = 0.40 μM) and even more potent than tamoxifen (2.2 μM). NS3728 accelerated channel inactivation at positive potentials. These results show that acidic di-aryl ureas constitute a promising starting point for the synthesis of potent inhibitors of VRAC.

Key words: VRAC — HEK cells — Chloride-channel blockers — Patch clamp — Electrophysiology — Volume — Swelling

Introduction

Volume-regulated anion channels (VRACs) comprise a class of chloride channels that contribute to the experimental regulatory volume decrease (RVD) response: Acute cell swelling in hypotonic media is counteracted by increased Cl^- and K^+ effluxes, which osmotically drive water efflux and restore cell volume (Hoffmann & Simonsen, 1989). Functional expression of VRACs seems to correlate closely with cell proliferation and migration in many cell types, possibly reflecting the need for subtle volume control during these processes. It has been suggested that VRAC inhibitors are anti-angiogenic agents having a therapeutic potential in cancer treatment (Chou, Shen & Wu, 1995; Voets et al., 1995; Shen et al., 2000; Ransom, O'Neil & Sontheimer, 2001; Wondergem et al., 2001). However, in vivo validation of this concept suffers strongly from the lack of non-toxic and metabolically stable blockers of VRACs.

In whole-cell patch-clamp experiments, VRACs are identified as a swelling-activated, outward-rectifying anion conductance with an Eisenman type I halide selectivity sequence. Despite years of investigation, the molecular nature of VRACs remains elusive, and it is questionable if it represents a single entity or a family of channels. The family of mammalian ClC channels was cloned in continuation of the identification of the skeletal muscle Cl^- channel (ClC-0) from *Torpedo* electroplaques, where it is highly expressed. Several genes, including ClC-2 and ClC-3, have been considered as the molecular correlate of the VRAC (Duan et al., 1997; Grunder et al., 1992; Paulmichl et al., 1992). However, it is now widely assumed that VRACs belong to a distinct family. One problem with Cl^- channels in general and VRACs in particular is the lack of selective high-affinity blockers, such as peptide constituents of animal or plant venoms to be used as tools in the purification and cloning process. A number of small organic molecules with VRAC blocking properties have been described, but they are neither very potent nor selective.

Correspondence to: P. Christophersen; email: pc@neurosearch.dk

In the present paper a novel class of simple, small molecule compounds (acidic substituted di-aryl-ureas) is compared with the classical Cl^- channel blockers DIDS, NPPB, and tamoxifen. The experiments were performed using VRACs endogenously expressed in HEK293. NS1652 and NS3623 have previously been shown to exhibit a potent block of the human erythrocyte Cl^- conductance in vitro. Furthermore, NS3623 has been tested in a transgenic mouse model for sickle cell anemia, where it blocked the erythrocyte Cl^- conductance in vivo and stabilized erythrocyte volume after oral administration (Bennekou et al., 2000, 2001). NS3749 and NS3728 are new compounds but belong to the same structural class as NS3623. The compounds NS1652, NS3623, NS3749 and NS3728 inhibited the VRAC with IC_{50}s of 97 μM, 1.8 μM, 1.4 μM and 0.40 μM, respectively. The structure–activity relation (SAR) of these four NeuroSearch (NS) compounds on the VRAC is distinct from the SAR obtained for the human erythrocyte Cl^- conductance, indicating that the activities can be separated. The observations may serve as a starting point for the synthesis of selective VRAC blockers as tools for cloning as well as for development of anti-angiogenesis drugs for in vivo proof-of-concept investigations.

Materials and Methods

Cell Culture

HEK293 cells (ATCC CRL-1573) were cultured in DMEM medium supplemented with 10% fetal calf serum and 2 mM Glutamax (Gibco, BRL). The cells were grown at 37°C in a humidified atmosphere of 5% CO_2 and 95% air. Cells were cultured in T25 flasks (Nunc) and when confluency reached 70–80%, the cells were trypsinized and seeded at 10–20% density in culture flasks or in Petri dishes containing the coverslips (Ø = 3.5 mm) used for the experiments.

Electrophysiology

All experiments were performed in the patch-clamp whole-cell configuration. For the pharmacological experiments, cover slips containing HEK293 cells were transferred to a custom-made experimental 15 μl recording chamber, positioned on an Olympus microscope (IX-70), and perfused with solution at a rate of 1 ml/min. For the ion-selectivity experiments a larger commercial chamber (RC-25F, Warner Instruments, Hamden, CT) was used. The reference electrodes consisted of an Ag/AgCl pellet that was connected via an agar salt bridge in the selectivity studies. Pipettes were pulled from borosilicate glass (Modulohm, Denmark) with a DPZ electrode puller (Zeitz Instruments, Germany) and placed in an electrode holder at the headstage of an EPC-9 amplifier (HEKA electronics, Germany). The EPC-9 amplifier was connected to a Macintosh G4 computer via an ITC-16 interface. Data was sampled at 3 times the filter cut-off frequency (3 kHz) with Pulse (HEKA electronics, Germany) and analyzed with IGOR software (WaveMetrics, Lake Oswego, OR). The pipettes, positioned by aid of a remotely controlled micromanipulator (Eppendorf, Germany), had a resistance of 1.5–3 MΩ when filled with the intracellular solution. The electrodes were zeroed just before touching a cell. Capacitative transients were automatically cancelled after establishment of the gigaseal, and again after entering the whole-cell configuration. The series resistance (R_S) recorded after breakthroughs to the whole-cell configuration were in the range of 2.5–5 MΩ. R_S was compensated 80%, updated between applications of voltage protocols, and never exceeded 8 MΩ. Currents were recorded either by application of a voltage step protocol from −100 to +100 mV with 20-mV step increases (from a holding potential of 0 mV; 200 ms duration) or by application of symmetric voltage ramps applied every 5 s (either ±100 or ±70 mV, 200 ms duration, *see* legends). Two isotonic extracellular solutions were used. The TEA-Cl solution contained (in mM): TEA-Cl (tetraethylammonium chloride) 142, $CaCl_2$ 2, $MgCl_2$ 1, and Tris 10 (pH 7.4) was primarily used for the investigation of the small background anion conductance in order to minimize all cation conductances and to avoid a possible Cl-channel block by HEPES. The TEA solution also allowed VRAC activation, but in this paper a slightly more physiological NaCl/CsCl solution was used. This solution contained (mM): NaCl 140, CsCl 4, $CaCl_2$ 2, $MgCl_2$ 1 and HEPES 10 (pH 7.4). For the ion-selectivity studies, NaCl was substituted with a corresponding concentration of NaI or Na-gluconate. The osmolalities of all extracellular solutions were in the range 280–300 mOsm when measured at The Advanced™ Osmometer (model 3D3, Advanced Instruments, Norwood, MA). The hypotonic solutions were made by adding water (0.25v:0.75v) to the isotonic solutions. All extracellular solutions were adjusted to pH 7.4 before use. The intracellular solutions used in the pipettes contained either 100 nM free calcium with (in mM): CsCl 110, Tris 10, EGTA 10, and $CaCl_2$ 5.17, or 1 μM free calcium with CsCl 110, Tris 10, EGTA 1, and $CaCl_2$ 0.955. Mg-ATP (4 mM) was added and the pH was adjusted to 7.20 with CsOH before use. The final Cs^+ concentration was 147 mM. The measured tonicity of the final intracellular solutions was in the same range as that of the extracellular solutions. The free calcium concentrations were calculated by Eqcal Software (Biosoftware, Cambridge, UK), taking into account the stability constants for all Ca^{2+}-, Mg^{2+}-, and H^+-binding ligands in the intracellular solution.

All compounds used were dissolved in 100% DMSO; except DIDS, which was dissolved in distilled water. The compounds were then diluted in the hypotonic solution to the required concentration. The final DMSO concentration did not exceed 0.1%, a concentration range without effect on the recorded currents. For all compounds concentration-response curves were established. Each compound was tested 2–8 times at each of the 4–8 different concentrations used. The mean I_c/I_0 ± SEM was plotted as a function of the concentration and these data points were used in the fitting routine. The IC_{50} values were calculated at −100 and +100 mV or −70 and +70 mV in order to address the question whether the block showed any voltage dependency.

Erythrocyte Experiments

Experiments were performed as previously described (Bennekou et al., 2000, 2001). In short, washed erythrocytes were suspended in a buffer-free extracellular salt solution containing the protonophore CCCP to monitor the erythrocyte membrane potential as change in the extracellular pH. With increasing concentrations of Cl-conductance blockers, valinomycin-induced hyperpolarizations were augmented and the fractional decrease in Cl conductance was calculated.

Fitting Procedures and Calculations

IC_{50} values were calculated from equilibrium concentration-response experiments. Data were fitted to a Hill equation of the following form:

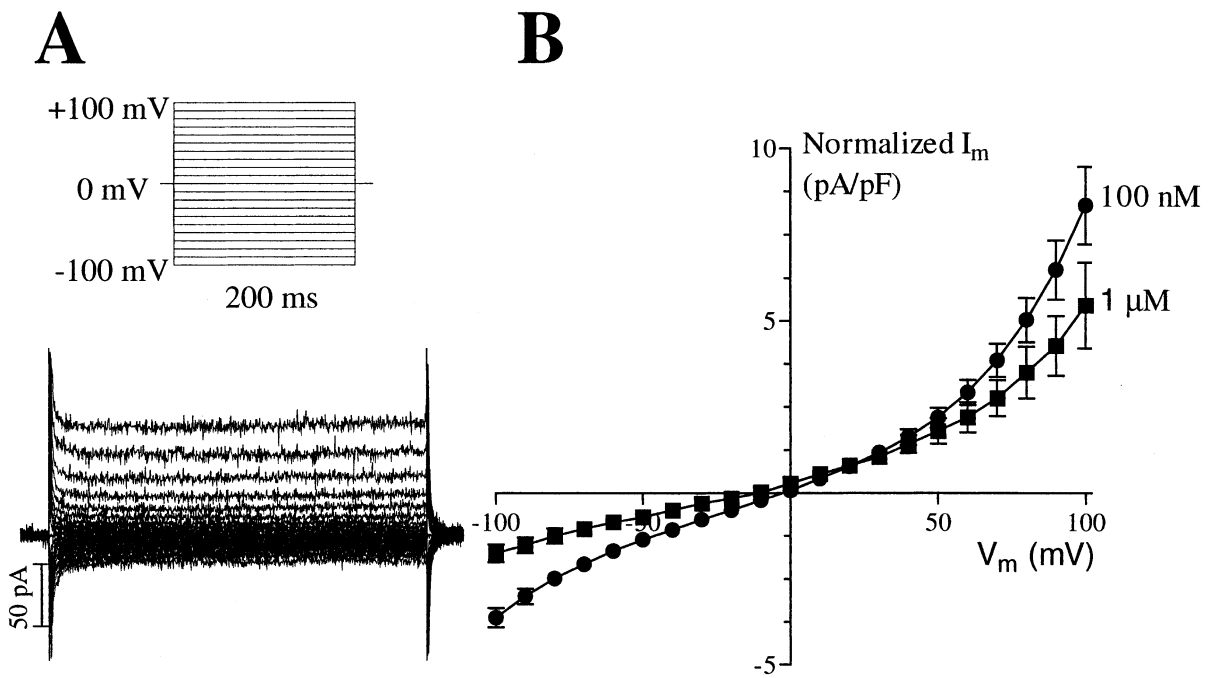

Fig. 1. Basal chloride currents in HEK293 cells. (*A*) *Upper panel* depicts the voltage-step protocol from −100 to +100 mV (200 ms duration) from a holding potential of 0 mV. *Lower panel* shows the corresponding currents recorded from a representative HEK293 cell in TEA-Cl solution. (*B*) Average of the normalized chloride currents (I_m) from 21 HEK293 cells recorded with an intracellular free [Ca^{2+}] of 100 nM and from 5 cells recorded with 1 μM free Ca^{2+}. The error bars represent the SEMs.

$$\frac{I_c}{I_o} = 1 - \frac{C^n}{C^n + (IC_{50})^n} \quad (1)$$

using a non-linear routine (Simplex). I_o is the unblocked current level, I_c is the stationary current level at the blocker concentration C, IC_{50} is the concentration giving 50% block and n is the Hill coefficient. The erythrocyte data were fitted to a similar equation.

For calculation of permeability ratios from shifts in reversal potentials (V_r) the following equation was used (Nilius et al., 1999):

$$\frac{P_x}{P_{Cl}} = \frac{C_{Cl}(n) \cdot \exp(-\Delta V_r \cdot F/RT) - C_{Cl}(S)}{C_x(S)} \quad (2)$$

where C is the concentration of anion (Cl or X) in the normal (n) or, respectively, the substituted (s) hypotonic solution. The reversal potential of the gluconate solution was corrected for a measured liquid junction potential of 4.5 mV.

Chemicals

DIDS (4,4-Diisothiocyanatostilbene-2,2-disulphonic acid), NPPB (5-Nitro-2-(3-phenyl-propylamino)-benzoic acid) and tamoxifen ((Z)-[4-(1,2-diphenyl-1-butenyl)phenoxy]-*N*,*N*-dimethylethanamine) were purchased from Sigma. NS1652 (2-[3-(3-trifluoromethyl-phenyl)-ureido]-benzoic acid), NS3623 (*N*-[4-bromo-2-(1*H*-tetrazol-5-yl)-phenyl]-*N*′-(3-trifluoromethyl-phenyl) urea), NS3749 (*N*-[4-Bromo-2-(1*H*-tetrazol-5-yl)-phenyl]-*N*′-(4-nitro-phenyl) urea) and NS3728 (*N*-[3,5-Bis(trifluoromethyl)-phenyl]-*N*′-[4-bromo-2-(1*H*-tetrazol-5-yl)-phenyl] urea) were synthesized at NeuroSearch A/S (Pederstrupvej 93, Ballerup, Denmark); for details see Christophersen & Pedersen, 1997, 1998; Dahl & Christophersen, 2000. Both the carboxylic acid compound (NS1652) and the tetrazoles (NS3623, NS3749, and NS3728) are acidic compounds (for a discussion of tetrazole chemistry, *see* Benson, 1947). Calculated pK_A values (ChemSketch, Advanced Chemistry Developments, Toronto, Canada), were 3.5 for NS1652 and 3.9 for the other NS-compounds.

All inorganic salts and buffer substances were from various commercial dealers and were of analytical grade or higher.

Statistics

Data are presented as mean ± SEM of n experiments and, where appropriate, have been analyzed using Student's t-test.

RESULTS

Evidence of VRAC Expression in Human Embryonic Kidney Cells (HEK293)

HEK293 cells express small whole-cell currents and are often chosen for heterologous expression of ion channels. Under conditions of blocked cation conductances (Fig. 1*A*) the *I-V* relation of the basal current was slightly outward-rectifying and reversed at −2 mV, which is in good agreement with the equilibrium potential for chloride (−5 mV). At 100 mV the normalized mean current was 8.3 ± 0.1 pA/pF (n = 21, Fig. 1*B*), corresponding to 98 ± 14 pA in a typical cell (12.0 ± 0.9 pF). These currents did not show any time dependency, as would have been expected for a voltage-dependent channel (Fig. 1*A*)

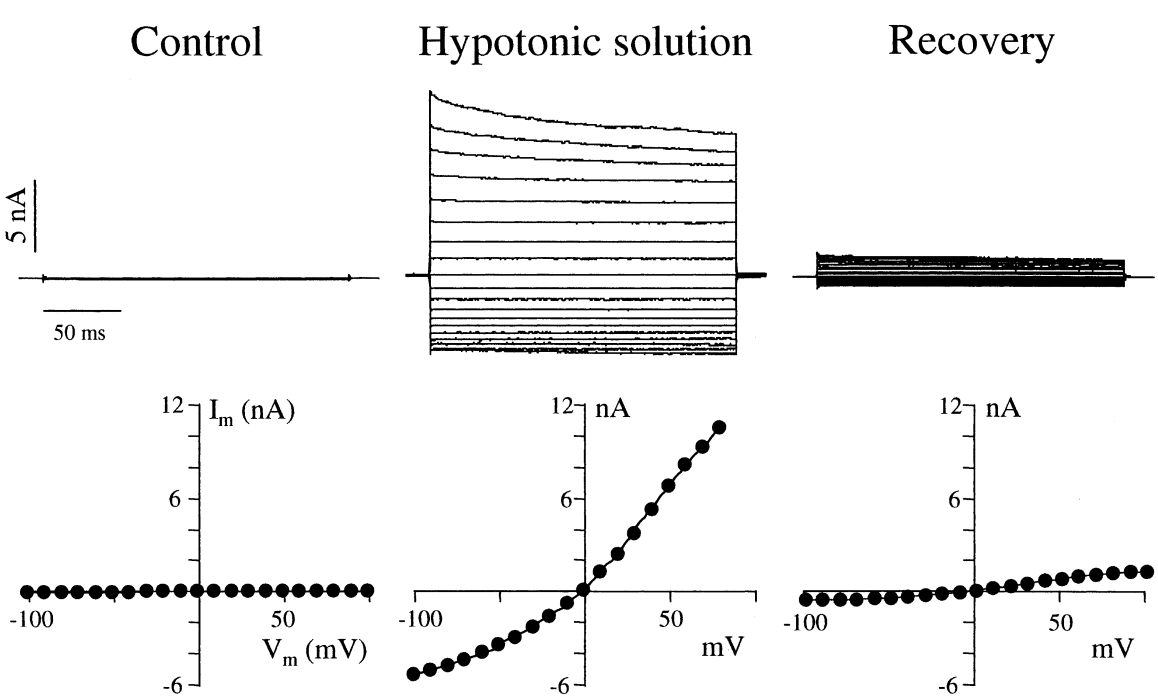

Fig. 2. VRACs in HEK293 cells. The *upper left panel* shows the chloride current in a representative HEK293 cell in NaCl/CsCl solution, and the *upper middle panel* shows the volume-regulated anion channels (VRACs) after application of hypotonic solution during 15 minutes. *Upper right panel* shows the recovery after application of isotonic solution during 60 minutes. *Lower panels* show the corresponding current (I_m)–voltage (V_m) relationships in each condition. The currents were measured at the end of the voltage step. The intracellular solution contained a free [Ca^{2+}] of 100 nM.

and the non-linearity thus probably results from instantaneous open-channel rectification. With 1 μM free Ca^{2+} in the pipette solution, the currents were similar to those obtained with 100 nM free Ca^{2+} (Fig. 1*B*). We conclude that HEK293 cells do not express a significant number of Ca^{2+}-activated Cl^--channels.

In contrast, by exposing the clamped HEK293 cell to a hypotonic extracellular solution (~220 mOsm compared to ~290 mOsm in the control NaCl/CsCl solution) a large increase in the conductance was observed (Fig. 2). The *I-V* relation measured from the step protocol shows that the swelling-induced current also exhibited instantaneous outward rectification, but at variance to the basal current it showed clear inactivation at potentials more positive than +40 mV. Some experiments were done without Mg-ATP in the pipette solution, which completely abolished the swelling-induced augmentation of the chloride conductance (*data not shown*). To establish the basic anion selectivity of the swelling-induced current, the permeability ratios of the iodide ion and gluconate *vs.* the chloride ion were established (Fig. 3*A*). For these studies the voltage protocol was changed from the step protocol employed in the experiments shown in Figs. 1 and 2 to a voltage-ramp protocol: A voltage ramp running from −70 mV to +70 mV in 200 ms was applied from a holding potential of 0 mV every 5 seconds (Fig. 3, *inset*). In the NaCl/CsCl solution a reversal potential of 6 ± 1 mV (n = 6) was recorded (theoretical E_{Cl} = 2 mV). Upon equimolar exchange of the extracellular Cl^- with I^- or gluconate (10 mM Cl^- remaining), distinct shifts in the reversal potentials towards more negative (ΔV_r = −8 ± 0.4 mV, n = 6), respectively positive potentials (ΔV_r = 37 ± 3 mV, n = 4), occurred. The observed changes in the reversal potentials correspond to a P_I/P_{Cl} of 1.4 and a $P_{gluconate}/P_{Cl}$ of 0.18. Overall these characteristics are similar to those found for volume-regulated anion channels (VRACs) in other cell types and the channel is thus referred to as VRAC in the subsequent paragraphs.

The development of VRAC current as a function of time was established (Fig. 3*B*). After obtaining the whole-cell configuration, the ramp currents were recorded in isotonic solution during 3 minutes before application of the hypotonic solution. The current typically started to increase about 1 minute after the exchange of the solution and reached a plateau after about 12–15 minutes ($t_{1/2}$ = 7 min). The plot of the mean current (measured at +100 mV) reveals a smooth, sigmoid, time-dependent activation curve, which may reflect cooperativity in the activation process of VRACs. In the hypotonic solution, the current at +100 mV reached 735 ± 44 pA/pF (n = 55) and at −100 mV it was approximately 2/3 smaller (251 ± 14 pA/pF).

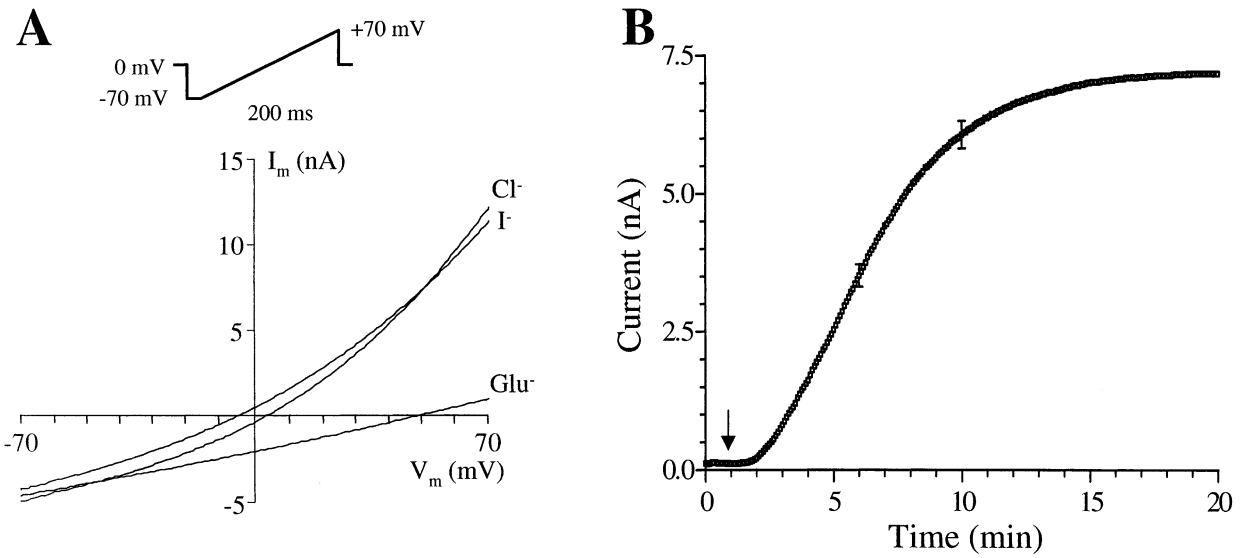

Fig. 3. Selectivity and time course of VRAC activation in HEK293 cells. (*A*) *Upper panel:* Ramp protocol applied every 5 seconds. *Lower panel:* Selectivity for gluconate (Glu^-) and iodide (I^-). After swelling and stabilization of current, extracellular Cl^- was partially exchanged (10 mM Cl^- remained) with gluconate or iodide. (*B*) The activation of VRACs as a function of time. The arrow indicates the time when perfusion with the hypotonic solution was initiated. Data were not normalized with respect to cell size and contained recordings from cells having 1.56 to 18.22 nA and being 5.35 to 22.46 pF, 10 minutes after the hypotonic solution was added. The symbols represent the mean values obtained from 55 cells and the error bars represent the SEM for selected points on the curve.

Pharmacological Characterization of VRACs in HEK293 Cells

For the pharmacological characterization of the VRACs in HEK293 cells the voltage-ramp protocol was used. Figure 4*A* shows the traces obtained in NaCl/CsCl (control; *C*) solution and in the hypotonic NaCl/CsCl solution (*VRAC*). In all pharmacological experiments the following procedure was followed: After a stable VRAC current was achieved, the hypotonic solution was changed to a hypotonic solution containing the desired concentration of the compound in question. When a new plateau current level was obtained, the compound was washed off by superfusion with the hypotonic solution alone. An example is shown in Fig. 4*B*, where the time course of VRAC activation (measured at −100 mV and at +100 mV from the ramp protocol) was measured and where DIDS and NPPB were tested. The cell was exposed to the hypotonic solution, as indicated by the solid bar, and during the periods indicated by open bars, the Cl^- channel blockers DIDS (30 μM) and NPPB (30 μM) were sequentially included in the hypotonic solution. DIDS reduced the current by 43 ± 8% ($n = 6$) at +100 mV (Fig. 4*B*), whereas no effect was observed at −100 mV, indicating a voltage-dependent action by DIDS. In contrast, NPPB reduced the inward and the outward currents to a similar degree (51 ± 22% at −100 mV and 44 ± 21% at +100 mV, respectively ($n = 4$)). Although the percentage of inhibition for both compounds was similar, DIDS reached steady state faster than NPPB. The effects of both compounds were completely reversible and the recovery showed similar differences in the kinetics as did the inhibition: faster for DIDS than for NPPB.

Figure 5 compiles the results obtained with the reference compounds. Figure 5*A* shows *I-V* ramps in the control situation and after application of a partially effective concentration of blocker. All compounds were tested at 5–7 concentrations and concentration–response curves were generated (Fig. 5*B*) based on current recordings at −100 mV as well as +100 mV in order to elucidate any possible voltage-dependent effects on affinity and/or Hill coefficients. The solid curves represent the best fit to Eq. 1. DIDS inhibited the VRACs with an IC_{50} value of 26 μM at +100 mV and 256 μM at −100 mV. The ten-times difference in the IC_{50} values represents the voltage-dependent block of this compound, whereas the Hill coefficient for inhibition by DIDS was independent of voltage (0.8 ± 0.1 at +100 mV and 0.9 ± 0.1 at −100 mV). In contrast, NPPB had similar IC_{50} values at +100 and −100 mV (21 and 27 μM, respectively) and the Hill coefficient was 1.4 ± 0.2. Finally, tamoxifen was tested. It is an anti-estrogen compound that is extensively used for the treatment of breast cancer. However, it is also a Cl^--channel blocker that has been used in studies of swelling-activated currents and related effects. Interestingly, the compound does exhibit some selectivity among VRACs from different cells. In most cases it is very potent (Wondergem et al., 2001; Chen et al., 2002) but in some cells it has no effect (Winpenny et al., 1996. Leaney, Marsh &

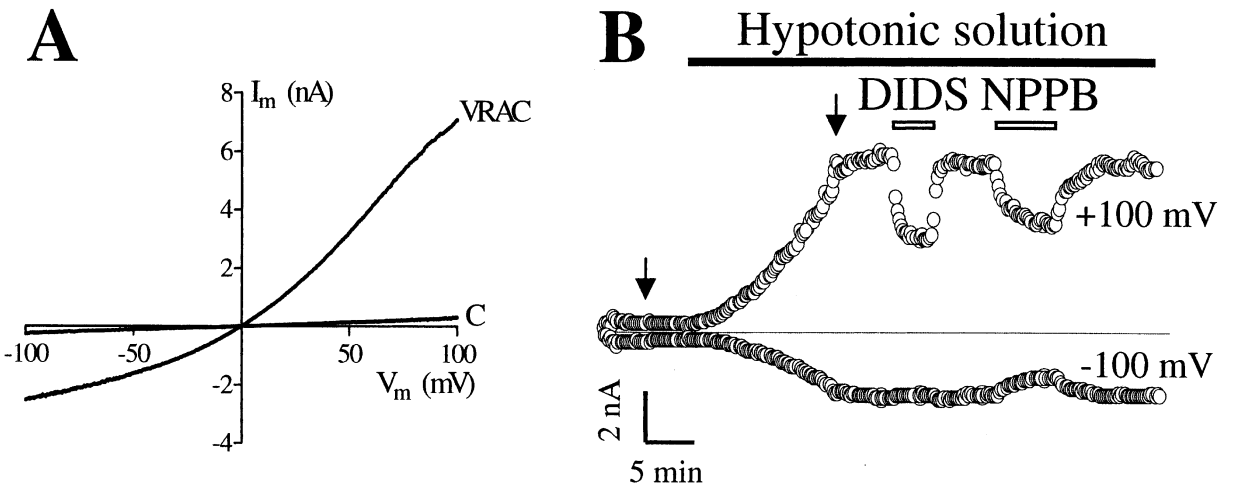

Fig. 4. Test of compounds on VRACs in HEK293 cells. (*A*) Currents (I_m) recorded in control condition (*C*) and after activation of the VRACs. (*B*) Representative experiment showing the current measured at −100 and +100 mV. After 4 min of basal current recording, the isotonic NaCl/CsCl solution was exchanged for the hypotonic NaCl/CsCl solution (*black bar*). When a plateau was reached, compounds were added (in this experiment, DIDS and NPPB at 30 μM). The arrows show the times at which the sweeps in *A* were taken.

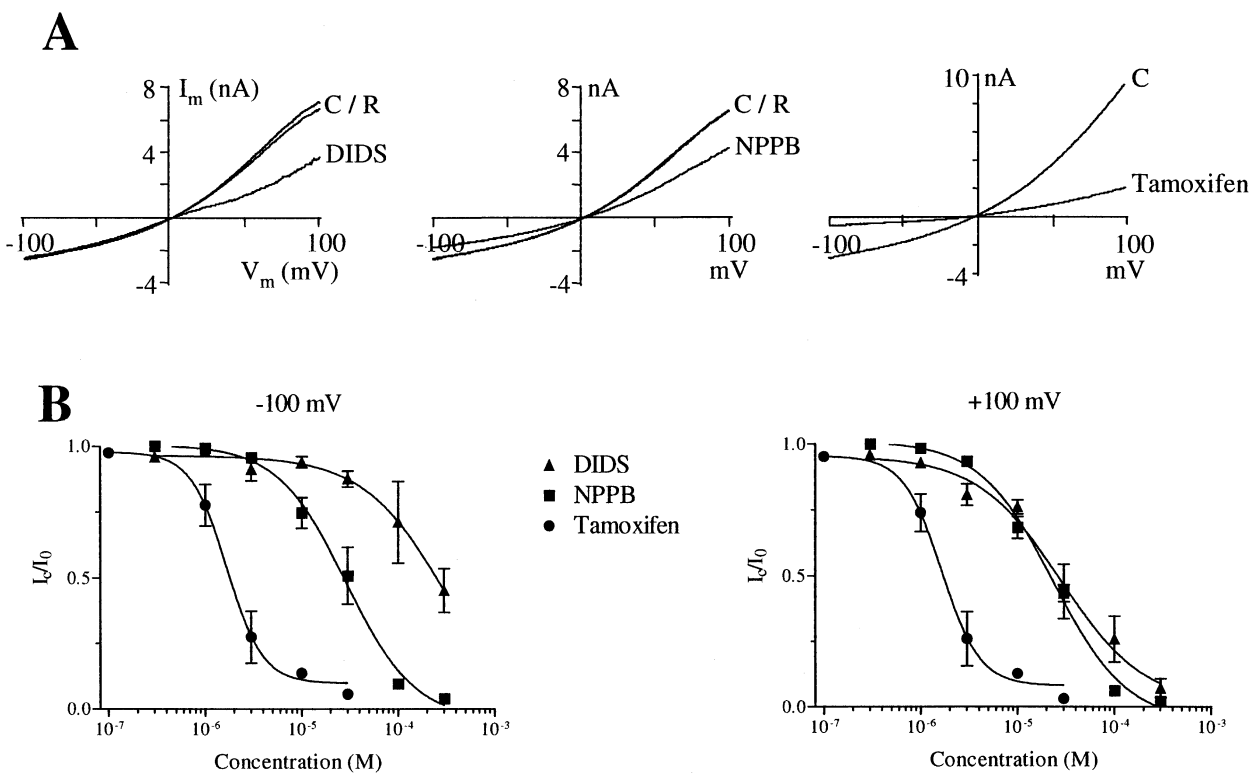

Fig. 5. Inhibition of VRACs by DIDS, NPPB and tamoxifen. (*A*) Current (I_m)–voltage (V_m) relationships obtained from the voltage-ramp protocol. *Left panel:* VRAC current in control conditions (*C*), after inhibition by DIDS (30 μM) and after recovery (*R*). *Middle panel:* VRAC current in control conditions, after inhibition by NPPB (30 μM) and after recovery. *Right panel:* VRAC current in control conditions and after inhibition by tamoxifen (10 μM). (B) *Left panel:* Fraction of current remaining (I_c/I_o) at −100 mV was plotted as a function of the concentration of the inhibitor (DIDS: ▲, NPPB: ■ and tamoxifen: ●). Each point is the average ± SEM of 2–6 experiments. *Right panel:* Fraction of current remaining at +100 mV was plotted as a function of the concentration of the inhibitor (DIDS: ▲, NPPB: ■ and tamoxifen: ●). Each point is the average ± SEM of 2–6 experiments. The IC_{50} values were calculated from the best fit of the average data to the Hill equation. At −100 mV the IC_{50} values were 256 μM, 27 μM and 2.6 μM for DIDS, NPPB and tamoxifen, respectively. At +100 mV the values were 26 μM, 21 μM and 2.2 μM, respectively.

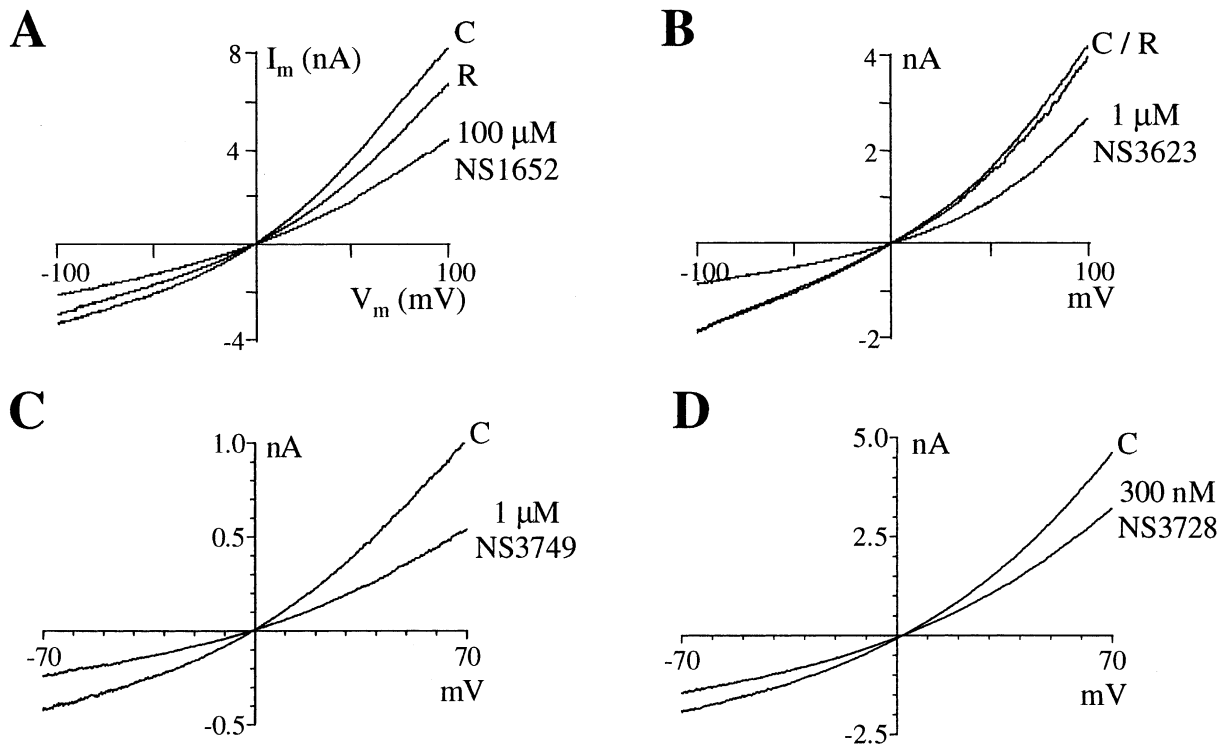

Fig. 6. Inhibition of VRACs by NS1652, NS3623, NS3749 and NS3728. Current (I_m)–voltage (V_m) relationships obtained from the voltage-ramp protocol. (*A*) VRAC current in control conditions (*C*), after inhibition by NS1652 and after recovery (*R*). (B) VRAC current in control conditions, after inhibition by NS3623 and after recovery. (*C*) VRAC current in control conditions and after inhibition by NS3749 in voltage-ramp protocol from −70 to +70 mV. (*D*) VRAC current in control conditions and after inhibition by NS3728 in voltage-ramp-protocol from −70 to +70 mV.

Brown, 1997; Mitchell et al., 1997). Therefore, it is important to profile the VRACs expressed in HEK293 cells with respect to tamoxifen sensitivity. With an IC_{50} value of 2.2 µM at +100 mV, tamoxifen was by far the most potent reference compound tested, and definitively categorized the HEK293 VRACs as tamoxifen-sensitive. The inhibition by tamoxifen did not show any voltage dependency (IC_{50} = 2.6 µM at −100 mV) and the Hill coefficient was 1.3 ± 0.1.

Inhibition of VRACs by Substituted Di-Aryl-Ureas

Figure 6*A, B, C* and *D* show representative effects of the various acidic di-aryl-ureas (NS1652, NS3623, NS3749 and NS3728) on VRAC ramp currents. Full concentration–response curves are plotted in Fig. 7. Obviously, NS1652, a carboxy derivative, is much less potent than the tetrazole derivatives NS3623, NS3749 and NS3728. At +100 mV, NS1652 blocks with an IC_{50} of 97 µM, whereas NS3623, NS3749 and NS3728 inhibited the VRAC current with IC_{50} values of 1.8 µM, 1.4 µM and 0.40 µM, respectively. Like NPPB and tamoxifen, the substituted di-aryl-ureas exhibited only modest, if any, voltage dependency (Table 1) and the Hill coefficients were close to 1.

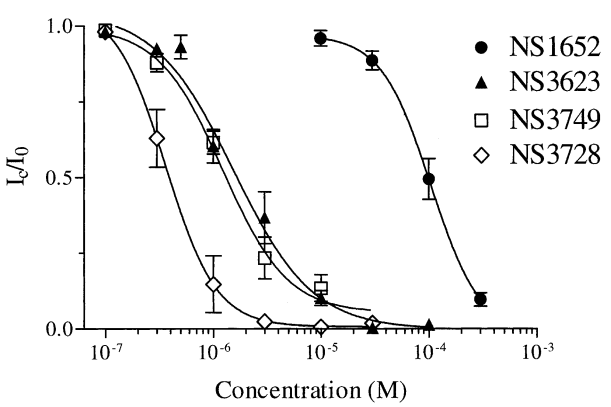

Fig. 7. Concentration response curves of VRAC inhibition by di-aryl-ureas. The fraction of outward current remaining was plotted as a function of the concentration of the inhibitor (NS1652: ●, NS3623: ▲, NS3749: □ and NS3728: ◇). Each point is the average ± SEM of 2–8 experiments. The IC_{50} values were calculated from the best fit of the average data to the Hill equation. On the outward current, the IC_{50} values were 97 µM, 1.8 µM, 1.4 µM and 0.40 µM for NS1652, NS3623, NS3749 and NS3728, respectively.

The affinity of both reference and NS compounds were also tested on the erythrocyte Cl conductance for comparison with the VRAC effect. Hyperpolarizations induced by addition of valinomycin to suspensions of erythrocytes were augmented by

sub-micromolar concentrations of DIDS and all NS compounds, whereas no effect of tamoxifen and NPPB was observed at 20 μM. Table 1 shows the obtained IC_{50} values.

Finally, in order to elucidate a possible effect on voltage-dependent channel inactivation by this new class of compounds, a swollen cell was voltage-clamped at −50 mV and the inactivation was induced by a 200 ms step to 80 mV (Fig. 8*A*). Application of 1 and 3 μM NS3728, the most potent compound, reversibly and dose-dependently (Fig. 8*B* and *C*) reduced both inward and outward currents, as expected. To high-light the effect on the channel inactivation, the peak amplitudes of the current traces obtained with blocker were rescaled to the peak of the control trace (Fig. 8*B*, *left panel*). Clearly, NS3728 dose-dependently accelerate voltage-dependent inactivation. Note also that the compound prolonged the time needed for recovery from inactivation (*compare* traces at −50 mV). From these experiments, we conclude that NS3623, NS3749 and NS3728 represent a new class of compounds that potently block VRACs in a voltage-independent and reversible manner.

Discussion

HEK293, a standard laboratory cell line, was investigated for endogenous expression of functional Cl^- channels by the whole-cell patch-clamp technique. Using extracellular and intracellular salt solutions, where the physiological relevant cations Na^+ and K^+ were exchanged with the impermeant TEA^+ and Cs^+, only a small Ca^{2+}-independent, outward-rectifying background Cl^- conductance was isolated. Absence of Ca^{2+}-activated Cl^- channels in HEK293 cells has previously been reported in a single-channel study by Zhu et al. (1998) and HEK293 cells have frequently been used for heterologous expression of proteins suggested to be calcium-activated chloride channels (Gruber et al., 1998; Fuller & Benos, 2000; Leverkoehne & Gruber, 2002).

In contrast, volume-regulated anion channels (VRACs) were abundently expressed. Upon swelling in hypotonic (75%) solution the currents activated with a sigmoid time dependence and reached a stable plateau level after about 10 min. During the swelling the total cell conductance (at 0 mV) increased from 1.3 ± 0.1 nS to 43 ± 3.1 nS (n = 55) as a consequence of channel activation. The VRACs were outward rectifiers exhibiting distinct inactivation at large positive potentials. Exchanging the extracellular solution to iodide- or gluconate salts showed that I^- was slightly more permeable than Cl^- (1.4 times) and that gluconate was considerably less permeable (0.18 times). These values are consistent with previously published values of VRACs from other cells (e.g., Voets et al., 1997). Intracellular ATP was an absolute requirement for channel activation.

The sigmoid time dependency of activation might solely indicate internal subunit conformational changes during activation. Thus the volume-dependent gating can in principle be modeled according to a classical cooperative model for channel activation. However, previous investigations on the mechanisms of activation of VRACs strongly points towards a very complicated sequence of events and the apparent cooperativity could also include elements of the activation cascade. This seems to involve the rho/rho-kinase pathway, permissive sub-micromolar concentrations of intracellular Ca^{2+}, as well as structural elements such as cytoskeleton and compartmentalization of signaling molecules in membrane caveolae (Szucs et al., 1996; Okada, 1997; Trouet et al., 1999, 2001, for reviews *see* Shaul & Anderson, 1998 and Eggermont et al., 2001).

The HEK293 VRACs were characterized pharmacologically using the standard Cl^- channel blockers DIDS, NPPB and tamoxifen as well as NS1652, NS3623, NS3749 and NS3728, which establish a new class (substituted acidic di-aryl-ureas) of Cl^--conductance blockers. DIDS exhibited a pronounced voltage-dependent inhibition of the VRACs, blocking outward currents more than inward currents. However, the effect was clearly concentration-dependent and detailed analysis of the concentration–response curves revealed that the voltage dependency could be ascribed entirely to an effect on the affinity of the block (IC_{50} = 26 μM at +100 mV *vs.* 256 μM at −100 mV) rather than changed Hill coefficients (n_H = 0.8 ± 0.1 at +100 mV *vs.* n_H = 0.9 ± 0.1 at −100 mV). In contrast, NPPB and tamoxifen both blocked voltage-independently, with tamoxifen being the most potent (21 μM *vs.* 2.2 μM). The di-aryl-ureas tested in this study were voltage-independent, reversible blockers of VRACs. In this series the most potent compound was NS3728 (0.40 μM), NS3623 and NS3749 were equipotent (1.8 μM and 1.4 μM, respectively), whereas NS1652 was a poor blocker (97 μM). NS3728 exhibited a distinct accelerating effect of the voltage-dependent inactivation of VRAC. NS1652 and NS3623 have previously been described as potent sub-micromolar blockers of the human erythrocyte Cl^- conductance (molecular identity uncertain) and were suggested to have potential in the prevention of red blood-cell dehydration in sickle-cell patients (Bennekou et al., 2000, 2001). The erythrocyte G_{Cl} block by the acidic di-phenyl-urea compounds was confirmed in the present study and further exemplified by the effect of NS3749 and NS3728. It is noteworthy that NS1652 is a relatively weak blocker of VRACs, whereas NS3623, NS3749 and NS3728 retain a high potency on this channel, meaning that the human erythrocyte Cl^- conductance and the VRACs carry different molecular enti-

Table 1. IC_{50} values for inhibition of VRACs and the human erythrocyte Cl conductance by classical Cl-channel blockers as well as the novel di-phenyl-ureas.

Compounds		HEK293 VRAC			Human red cell G_{Cl}
Structure	Name	IC_{50} (μM) Inward current	IC_{50} (μM) Outward current	Ratio	IC_{50} (μM)
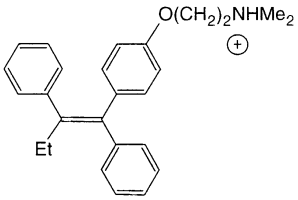	Tamoxifen	2.6	2.2	1.2	> 20
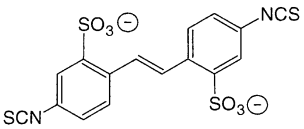	DIDS	256	26	9.8	Irreversible
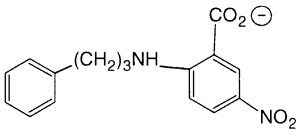	NPPB	27	21	1.3	> 20
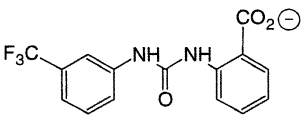	NS1652	125	97	1.3	1.6
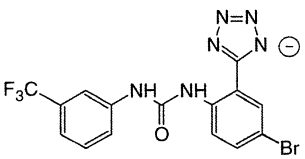	NS3623	1.8	1.8	1.0	0.6
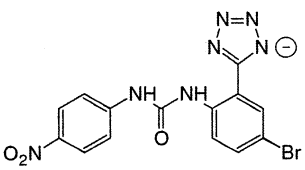	NS3749	1.9	1.4	1.4	1.4
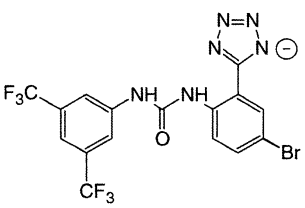	NS3728	0.46	0.40	1.1	0.6

The values for VRAC inhibition were obtained for the inward and the outward currents, respectively, and the ratio of IC_{50In}/IC_{50Out} were calculated to evaluate any voltage-dependent block by the compounds. The erythrocyte values were obtained under electrogenic K^+ and Cl^- efflux conditions from suspensions of human red blood cells (3.1% cytocrit), which is equivalent to an inward Cl^- current at negative membrane potentials. The compounds are shown as charged structures, which is the predominant form at pH = 7.4.

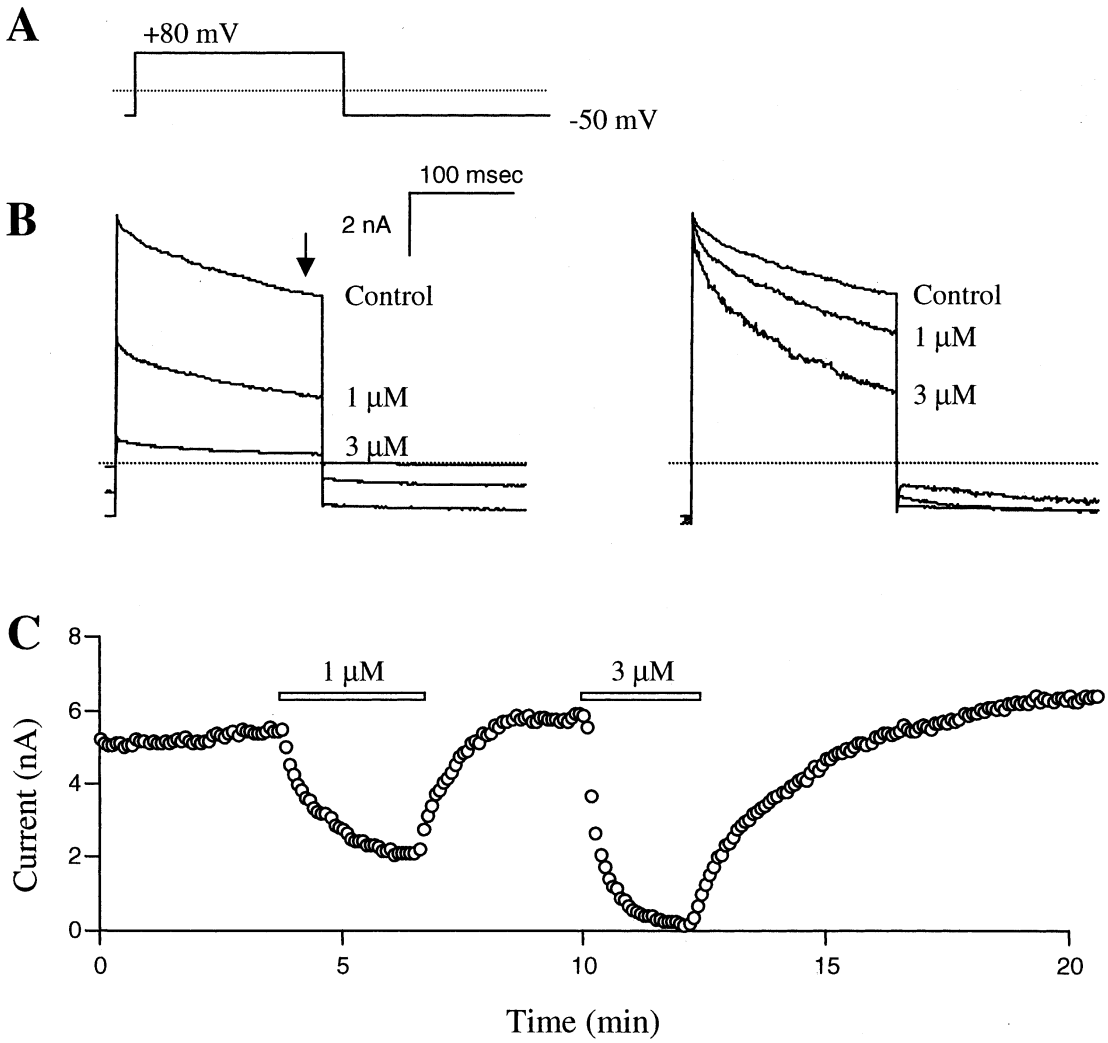

Fig. 8. Effect of NS3728 on VRAC inactivation. (*A*) Voltage protocol consisting of a holding potential of −50 mV followed by a voltage step to +80 mV for 200 msec. (*B*) *Left panel:* Current in hypotonic solution (*Control*), and with 1 μM and 3 μM of NS3728. The arrow shows where the current was taken for panel *C*. *Right panel:* The control trace is the same as in the left panel. The 1 and 3 μM traces have been multiplied by a factor in order to obtain a maximal outward current equal to the control current so as to highlight the increased rate of inactivation. (*C*) Current at +80 mV as a function of time. The bars represent the time during which NS3728 was applied (1 and 3 μM). Identical results were obtained in two additional experiments ($n = 3$).

ties at the blocker site. In various cell types, VRACs have been shown to be inhibited by numerous different chemical structures, being only remotely related to each other: A structural unifying concept of the classical Cl^--channel blockers like NPPB, niflumic acid, and DIDS is that they are di-aromatic, 2-substituted acids linked by various chains. However, hitherto this chemical class has not produced very potent VRAC blockers. Tertiary amines, like tamoxifen and verapamil and various phenol-derivatives like gossypol (for a review, *see* Nilius et al., 1999) are also VRAC blockers and the most potent entities are found in these groups. For compounds containing an alkaline nitrogen it has been argued that the uncharged form of the molecules inhibit the channel (Voets, Droogmans & Nilius, 1996; Maertens et al., 2001), possibly indicating that the binding site for these compounds is exposed to the lipid phase of the membrane.

The fact that VRACs are blocked by structurally very different compounds raises the concern that some of the effects may be indirectly caused by interference with diverse levels in the activation cascade. However, since the di-aromatic substituted acids are all nearly 100% negatively charged at pH = 7.4 (pK_A values usually 3–4, *see* Materials and Methods), it is tempting to assume that the negative group mimics an anion that would normally pass through the channel. Therefore, these compounds probably interact with the pore region, perhaps even with residues near the selectivity filter. This is consistent with the fact that we find instantaneous volt-

age-dependent blockers (i.e., DIDS) in this group. It is also possible that the increased rate of voltage-dependent inactivation, shown for niflumic acid and NPPB (Voets et al., 1997) and for NS3728 (present study), may reflect blocker exclusion of ions from an externally-facing, gating-regulatory site in the permeation pathway.

The main problem with the standard acidic diaryls known and characterized as Cl^--channel blockers so far is their very low potency, usually ranging from 10–1000 μM, which makes them very bad tools for VRAC purification and completely excludes them as in vivo active drugs. The new compounds shown here are chemically different from the classical Cl^- blockers in two important aspects: 1) They use the tetrazole moiety as acidic group rather than carboxylic or sulfonic acid groups and 2) they carry the urea moiety as a linker between the two aromatic centers of the molecule. This combination produces compounds that are significantly more potent VRAC blockers than the standard compounds and the results obtained with NS3728 give promise that further optimization will reveal low-nM-potency VRAC blockers. A systematic study on the structure–activity relationship for potency, voltage dependency and inactivation of block is urgently needed to explore this further.

It has previously been shown (Bennekou et al., 2000, 2001) that NS3623 has good in vivo pharmacodynamic properties, i.e., long-lasting erythrocyte Cl^--conductance block upon single oral doses and normalization of sickle-cell volume in normal and transgenic mice as well as low toxicity (3 weeks dosing). Further, NS3623 exhibited no activity (10 μM) on 60 different receptor-binding assays, including vascular endothelial growth factor (VEGF). This is promising for the structurally related new potent blocker of VRACs, NS3728, and this compound or a close analogue may be valuable in the elucidation of the role of VRACs as a pharmaceutical target for inhibition of angiogenesis and cancer in vivo.

Vibeke Meyland-Smith is gratefully acknowledged for her expert assistance with patch-clamp electrophysiology. N. Helix was financed by the European Community via the Marie Curie Industrie Host Fellowship (QLK-CT-2000-60044).

References

Bennekou, P., de Franceschi, L., Pedersen, O., Lian, L., Asakura, T., Evans, G., Brugnara, C., Christophersen, P. 2001. Treatment with NS3623, a novel Cl-conductance blocker, ameliorates erythrocyte dehydration in transgenic SAD mice: a possible new therapeutic approach for sickle cell disease. *Blood* **97:**1451–1457

Bennekou, P., Pedersen, O., Moller, A., Christophersen, P. 2000. Volume control in sickle cells is facilitated by the novel anion conductance inhibitor NS1652. *Blood* **95:**1842–1848

Benson, R. 1947. The chemistry of the tetrazoles. *Chem. Rev.* **41:**1–65

Chen, L., Wang, L., Zhu, L., Nie, S., Zhang, J., Zhong, P., Cai, B., Luo, H., Jacob, T.J. 2002. Cell cycle-dependent expression of volume-activated chloride currents in nasopharyngeal carcinoma cells. *Am. J. Physiol.* **283:**C1313–1323

Chou, C.Y., Shen, M.R., Wu, S.N. 1995. Volume-sensitive chloride channels associated with human cervical carcinogenesis. *Cancer Res.* **55:**6077–6083

Christophersen, P., Pedersen, O. NeuroSearch A/S. PCT/EP97/02723[WO 97/45400]. 1997. Denmark. Ref Type: Patent

Christophersen, P., Pedersen, O. NeuroSearch A/S. PCT/DK98/00162[WO 98/47879]. 1998. Denmark. Ref Type: Patent

Dahl, B.H., Christophersen, P. NeuroSearch A/S. PCT/DK99/00575[WO 00/24707]. 2000. Denmark. Ref Type: Patent

Duan, D., Winter, C., Cowley, S., Hume, J.R., Horowitz, B. 1997. Molecular identification of a volume-regulated chloride channel. *Nature* **390:**417–421

Eggermont, J., Trouet, D., Carton, I., Nilius, B. 2001. Cellular function and control of volume-regulated anion channels. *Cell Biochem. Biophys.* **35:**263–274

Fuller, C.M., Benos, D.J. 2000. Ca^{2+}-activated Cl^- channels: A newly emerging anion transport family. *News Physiol. Sci.* **15:**165–171

Gruber, A.D., Elble, R.C., Ji, H.L., Schreur, K.D., Fuller, C.M., Pauli, B.U. 1998. Genomic cloning, molecular characterization, and functional analysis of human CLCA1, the first human member of the family of Ca^{2+}-activated Cl^- channel proteins. *Genomics* **54:**200–214

Grunder, S., Thiemann, A., Pusch, M., Jentsch, T.J. 1992. Regions involved in the opening of ClC-2 chloride channel by voltage and cell volume. *Nature* **360:**759–762

Hoffmann, E.K., Simonsen, L.O. 1989. Membrane mechanisms in volume and pH regulation in vertebrate cells. *Physiol. Rev.* **69:**315–382

Leaney, J.L., Marsh, S.J., Brown, D.A. 1997. A swelling-activated chloride current in rat sympathetic neurones. *J. Physiol.* **501:**555–564

Leverkoehne, I., Gruber, A.D. 2002. The murine mCLCA3 (alias gob-5) protein is located in the mucin granule membranes of intestinal, respiratory, and uterine goblet cells. *J. Histochem. Cytochem.* **50:**829–838

Maertens, C., Droogmans, G., Chakraborty, P., Nilius, B. 2001. Inhibition of volume-regulated anion channels in cultured endothelial cells by the anti-oestrogens clomiphene and nafoxidine. *Br. J. Pharmacol.* **132:**135–142

Mitchell, C.H., Zhang, J.J., Wang, L., Jacob, T.J. 1997. Volume-sensitive chloride current in pigmented ciliary epithelial cells: role of phospholipases. *Am. J. Physiol.* **272:**C212–C222

Nilius, B., Voets, T., Eggermont, J., Droogmans, G. 1999. VRAC: A multifunctional volume-regulated anion channel in vascular endothelium. *In*: Chloride Channels, ed. Kozlowski., R., pp. 47–63. Isis Medical Media, Oxford, UK.

Okada, Y. 1997. Volume expansion-sensing outward-rectifier Cl^- channel: fresh start to the molecular identity and volume sensor. *Am. J. Physiol.* **273:**C755–C789

Paulmichl, M., Li, Y., Wickman, K., Ackerman, M., Peralta, E., Clapham, D. (1992). New mammalian chloride channel identified by expression cloning. *Nature* **356:**238–241

Ransom, C.B., O'Neal, J.T., Sontheimer, H. 2001. Volume-activated chloride currents contribute to the resting conductance and invasive migration of human glioma cells. *J. Neurosci.* **21:**7674–7683

Shaul, P.W., Anderson, R.G. 1998. Role of plasmalemmal caveolae in signal transduction. *Am. J. Physiol.* **275:**L843–L851

Shen, M.R., Droogmans, G., Eggermont, J., Voets, T., Ellory, J.C., Nilius, B. 2000. Differential expression of volume-regulated anion channels during cell cycle progression of human cervical cancer cells. *J. Physiol.* **529:**385–394

Szucs, G., Heinke, S., Droogmans, G., Nilius, B. 1996. Activation of the volume-sensitive chloride current in vascular endothelial cells requires a permissive intracellular Ca^{2+} concentration. *Pfluegers Arch.* **431:**467–469

Trouet, D., Hermans, D., Droogmans, G., Nilius, B., Eggermont, J. 2001. Inhibition of volume-regulated anion channels by dominant-negative caveolin-1. *Biochem. Biophys. Res. Commun.* **284:**461–465

Trouet, D., Nilius, B., Jacobs, A., Remacle, C., Droogmans, G., Eggermont, J. 1999. Caveolin-1 modulates the activity of the volume-regulated chloride channel. *J. Physiol.* **520:**113–119

Voets, T., Droogmans, G., Nilius, B. 1996. Potent block of volume-activated chloride currents in endothelial cells by the uncharged form of quinine and quinidine. *Br. J. Pharmacol.* **118:**1869–1871

Voets, T., Droogmans, G., Nilius, B. 1997. Modulation of voltage-dependent properties of a swelling-activated Cl^- current. *J. Gen. Physiol.* **110:**313–325

Voets, T., Szucs, G., Droogmans, G., Nilius, B. 1995. Blockers of volume-activated Cl^- currents inhibit endothelial cell proliferation. *Pfluegers Arch.* **431:**132–134

Winpenny, J.P., Mathews, C.J., Verdon, B., Wardle, C.J., Chambers, J.A., Harris, A., Argent, B.E., Gray, M.A. 1996. Volume-sensitive chloride currents in primary cultures of human fetal vas deferens epithelial cells. *Pfluegers Arch.* **432:**644–654

Wondergem, R., Gong, W., Monen, S.H., Dooley, S.N., Gonce, J.L., Conner, T.D., Houser, M., Ecay, T.W., Ferslew, K.E. 2001. Blocking swelling-activated chloride current inhibits mouse liver cell proliferation. *J. Physiol.* **532:**661–672.

Zhu, G., Zhang, Y., Xu, H., Jiang, C. 1998. Identification of endogenous outward currents in the human embryonic kidney (HEK293) cell line. *J. Neurosci. Methods* **81:**73–83